Insulin sensitivity and nutrient utilisation in skeletal muscle

by

Yan Yan Lam

Thesis submitted in fulfilment of the requirement for
the Degree of Doctor of Philosophy

Discipline of Medicine
School of Medicine
Faculty of Health Sciences
University of Adelaide, South Australia, Australia

November 2009

Chapter 4: Effect of secretory factors from adipose tissue on insulin-stimulated glucose uptake in skeletal muscle cells

4.1 Introduction

Insulin resistance is integral to the pathophysiology of obesity-related metabolic abnormalities (Reaven 2005). Not all obese individuals are insulin-resistant. A subgroup of obese individuals, accounting for ~ 20% of the obese population, remain insulin-sensitive and maintain a normal metabolic profile (Rasouli et al. 2007). The pattern of fat distribution is a key determinant of individual metabolic risk. The accumulation of visceral fat as opposed to subcutaneous fat confers an increased risk of the metabolic syndrome in both men and women irrespective of BMI (Goodpaster et al. 2005). In contrast, greater skeletal muscle mass and strength is protective of the risks (Atlantis et al. 2009). The accumulation of visceral fat is associated with decreased insulin sensitivity in both non-obese and obese individuals (Wajchenberg 2000; Karelis et al. 2004) and accounts for ~ 50% of the variance in insulin sensitivity (Kelley et al. 2000; Cnop et al. 2002). Skeletal muscle is the predominant site of glucose disposal and *in vivo* there is an inverse relationship between visceral fat mass and insulin-stimulated glucose disposal in skeletal muscle (Colberg et al. 1995; Virtanen et al. 2005).

The mechanisms by which visceral adipose tissue induces insulin resistance include an increased release of free fatty acids directly into the portal venous system as a result of the high lipolytic activity of the visceral adipocytes (Wajchenberg 2000) and an increased production of pro-inflammatory cytokines from adipocytes and/or activated macrophages located in the stromal component of visceral fat (de Luca and Olefsky

2008). The molecular mechanisms involved in adipose tissue-mediated insulin resistance in skeletal muscle and the reasons for the differences of the effects between subcutaneous and visceral adipose tissues are yet to be fully elucidated.

Epidemiological data indicate an association between chronic activation of pro-inflammatory signalling pathways and decreased insulin sensitivity. Circulating levels of inflammatory markers are increased in individuals with type 2 diabetes mellitus, insulin resistance or the metabolic syndrome (Crook 2004). In a prospective case-control study, elevated plasma levels of IL-6 and C-reactive protein have been shown to be associated with an increased risk of developing type 2 diabetes, independent of BMI, physical activity and other lifestyle factors (Hu et al. 2004). The hypoglycaemic and insulin-sensitising effect of salicylates, drugs commonly used to treat inflammatory conditions such as rheumatic fever and rheumatoid arthritis, further supports the role of inflammation in the development of insulin resistance. In genetically obese rodents and type 2 diabetic patients, the short-term administration of high-dose aspirin reduced fasting and postprandial blood glucose and insulin-stimulated peripheral glucose uptake (Yuan et al. 2001; Hundal et al. 2002). In rodents the effect was associated with an increased activation of insulin signalling components in liver and skeletal muscle (Yuan et al. 2001).

The activation of NFκB, a transcription factor which induces the expression of genes encoding proteins involved in immune and inflammatory reactions, may be the point of convergence of the effect of pro-inflammatory cytokines on mediating insulin resistance (Lee and Burckart 1998). Under basal conditions, NFκB is bound to the inhibitor protein inhibitor kappa B (IκB) and remains in its inactive form in the cytoplasm. When

phosphorylated by its upstream kinase inhibitor of kappa B kinase (IKK), IκB undergoes proteosomal degradation and thus releases NFκB for translocation to the nucleus and activates gene expression (Shoelson et al. 2003). Cytoplasmic IκB content is inversely related to NFκB DNA binding activity and thus a low IκB abundance indicates the activation of the IκB/NFκB pathway (Karin and Ben-Neriah 2000). IκB protein expression is associated with insulin-stimulated glucose disposal in human skeletal muscle and type 2 diabetic patients have been shown to have 60% lower intramuscular IκB content when compared to healthy controls (Sriwijitkamol et al. 2006). In mice fed with a high-fat diet, insulin resistance was increased by 2.5-fold, an effect that was associated with a 2-fold increase in hepatic NFκB activity (Cai et al. 2005).

The role of the IKK/IκB/NFκB pathway in mediating insulin resistance has been further illustrated in studies in transgenic mice. Mice with constitutively active IKKβ in the liver exhibited a type 2 diabetes phenotype including hyperglycaemia and moderate systemic insulin resistance (Cai et al. 2005). Conversely, mice with hepatic IKKβ deletion had lower postprandial blood glucose and insulin levels when compared to the controls during high-fat feeding (Arkan et al. 2005). IL-1β-induced reduction in insulin-stimulated insulin receptor activation and the association of the p85 subunit of PI3K with IRS-1 was completely prevented in primary hepatocytes infected with a specific inhibitor of NFκB activation (Arkan et al. 2005). In skeletal muscle, silencing IKKβ gene expression abolished the inhibitory effect of TNF-α on insulin-stimulated glucose uptake in primary human myotubes (Austin et al. 2008). An association between IKK activity and the inhibition of insulin-stimulated tyrosine phosphorylation of IRS-1 has been consistently demonstrated *in vivo* and *in vitro* (de Alvaro et al. 2004; Cai et al. 2005). Nevertheless, mechanisms downstream of the IKK/IκB/NFκB pathway by which insulin

resistance occurs and the role of individual pro-inflammatory cytokines remain to be fully elucidated.

Recent studies suggest that the activation of the mammalian target of rapamycin complex 1 (mTORC1) may be the molecular link between inflammation and insulin resistance. mTORC1 is a nutrient sensor which, when activated, promotes insulin resistance in a state of nutrient satiation (Um et al. 2006). A constitutively activated mTORC1 signalling pathway has been shown in the skeletal muscle of *ob/ob* mice (Miller et al. 2008) and of high-fat diet-fed obese rats (Khamzina et al. 2005). mTORC1 may attenuate insulin signalling by activating S6K1, which phosphorylates IRS-1 at several serine residues and disrupts its interaction with the insulin receptor and/or p85 subunit of PI3K (Dann et al. 2007). mTORC1 is activated by various mechanisms, which include the well-established negative feedback loop of insulin, in which the activation of the class I PI3K-Akt pathway dissociates the tuberous sclerosis complex (TSC)-1/TSC-2 complex which, via activating the GTP-bound Rheb, increases mTORC1 activity (Dann et al. 2007), as well as phosphorylation by the class III PI3K in response to branch-chain amino acids (Nobukuni et al. 2005). In 3T3-L1 preadipocytes, TNF-α-induced serine phosphorylation of IRS-1 was associated with an activation of mTORC1, an effect abolished by aspirin (Gao et al. 2003). Insulin-stimulated tyrosine phosphorylation of IRS-1 and glycogen synthesis in HepG2 cells were ameliorated by IL-6 but were restored to that of the controls by rapamycin, a specific inhibitor of mTORC1 activation (Kim et al. 2008). These data suggest that the inhibitory effect of pro-inflammatory cytokines on insulin sensitivity may be mediated by both the NFκB and mTORC1 signalling pathways. The direct link, if any, between the activation of NFκB and mTORC1 in skeletal muscle insulin resistance remains largely unclear.

In the present study, I aimed to determine the depot-specific effects of adipose tissue on insulin sensitivity in skeletal muscle *in vitro* and the mechanisms involved using the adipose tissue-conditioned media (Chapter 3). I hypothesised that:

1. The net effect of secretory factors from IAB but not SC fat would inhibit insulin-stimulated glucose uptake in L6 myotubes.
2. The IAB fat-induced insulin resistance would be reversed by inhibiting the activation of either NFκB or mTORC1.

4.2 Materials and methods

4.2.1 Adipose tissue-conditioned medium (CM)

SC and IAB adipose tissue explants were obtained from four obese non-diabetic patients (three female and one male; Table 4.1) undergoing gastric bypass surgery for the treatment of morbid obesity. CM was generated as described in Section 2.3 and that collected after 48 h of culture was used in the present study (Section 3.3.2).

Table 4.1. Clinical characteristics of tissue donors (n = 4).

	Mean ± SD	Range
Age (yr)	62.5 ± 8.2	51 – 74
Body Mass Index (kg/m^2)	51.3 ± 5.1	45.3 – 56.9
Fasting glucose (mmol/L)	4.9 ± 0.8	4.0 – 5.8
Fasting insulin (mU/L)	8.5 ± 7.2	3.8 – 21.0
HbA1c (%)	5.9 ± 0.2	5.5 – 6.1
Fasting cholesterol (mmol/L)	4.8 ± 1.2	3.1 – 6.6
Fasting triglycerides (mmol/L)	1.7 ± 0.9	0.8 – 3.2

4.2.2 Cytokine and fatty acid profiling in the adipose tissue-conditioned medium

The concentrations of adiponectin, IL-1β, IL-6, IL-8, TNF-α, resistin, PAI-1 (total) in CM from IAB and SC fat were determined using a Human Adipocyte Linco*plex* Kit and leptin level was measured by ELISA (Section 2.5). Fatty acid profile in CM from both fat depots was determined using gas chromatography (Section 2.6).

4.2.3 Rapamycin and pyrrolidinedithiocarbamate (PDTC)

Rapamycin and PDTC, inhibitors of mTORC1 and NFκB activation respectively, were used to determine the role of mTORC1 and NFκB signalling pathways in insulin resistance in skeletal muscle cells. Rapamycin inhibits mTORC1 function by forming a complex with FKBP12 which then interacts with the FRB domain in mTORC1 to alter its ability to phosphorylate the downstream substrates (Huang et al. 2003). PDTC is an antioxidant which prevents the degradation of IκBα and therefore attenuates the translocation of NFκB from the cytoplasm to the nucleus (Cuzzocrea et al. 2003).

Stock solutions of rapamycin (Sigma-Aldrich #R8781; 10 μM) and PDTC (Sigma-Aldrich #P8765; 0.05 M) were prepared in DMSO and sterile deionised water respectively and stored at -20°C until use. The optimal concentrations of rapamycin and PDTC to reverse insulin resistance in L6 myotubes were determined by dose-response trials with the selected ranges based on doses used in previous studies (Sen et al. 1997; Sipula et al. 2006). Rapamycin (0 – 40 nM) and PDTC (0 – 400 μM) was added to myotubes 30 min prior to CM and was retained during the culture.

4.2.4 Neutralisation of IL-6 in the adipose tissue-conditioned medium

The direct involvement of IL-6 in IAB fat-induced insulin resistance was determined by neutralising the biological activity of IL-6 in the CM. The optimal concentration of a human-specific anti-IL-6 antibody (Sigma-Aldrich #I2143) to increase insulin-stimulated glucose uptake in L6 myotubes cultured with CM from IAB fat was determined by a dose-response trial (0 – 40 μg/ml) with the selected range based on previous studies (Weigert et al. 2004; Jove et al. 2005). The antibody was diluted with α-MEM supplemented with 1% BSA (w/v) according to manufacturer's instructions. The antibody was added to the myotubes together with the CM. The concentration of BSA was kept at 1% (w/v) in all treatment groups.

4.2.5 Glucose uptake

L6 cells were cultured on 12-well plates (Section 2.2.1). Myotubes were incubated with CM (concentrations 1:2 – 1:128) for 6 h, with or without the presence of rapamycin/PDTC/anti-IL-6 antibody in the corresponding experimental groups, in an atmosphere of 5% CO_2 at 37°C. The plate content was aspirated afterwards. Myotubes were then incubated with or without 100 nM insulin for 30 min, which was followed by the measurement of 2-deoxy-D-[^{3}H] glucose uptake as described in Section 2.7.

4.2.6 Data analysis

Data are expressed as means ± SEM. Statistical analyses were performed by Student's *t* test, one-way or two-way ANOVA with Bonferroni post hoc tests to compare differences between experimental conditions using the GraphPad Prism Program. Significance was accepted at $P < 0.05$.

4.3 Results

4.3.1 Cytokine profiling in the adipose tissue-conditioned medium

The concentration of TNF-α of two CM samples fell below the detection limit (0.1 pg/ml) and so their values were approximated by half of the detectable value (i.e., 0.05 pg/ml) and then the dataset was analysed as per normal (Clarke 1998).

The concentrations of IL-6 and IL-8 in CM from IAB fat were 15-fold ($P < 0.05$; Figure 4.1A) and 8-fold ($P < 0.05$; Figure 4.1B) higher compared to that from SC fat respectively. In CM from IAB as compared to SC fat, the concentration of adiponectin (75%; $P = 0.13$; Figure 4.1C) was lower while those of TNF-α (320%; $P = 0.11$; Figure 4.1D), resistin (223%; $P = 0.13$; Figure 4.1E) and PAI-1 (153%; $P = 0.07$; Figure 4.1F) were higher. The concentration of leptin in CM from IAB and SC depots was similar (Figure 4.1G). IL-1β was undetectable in all CM samples from both depots (minimum detectable concentration 0.1 pg/ml).

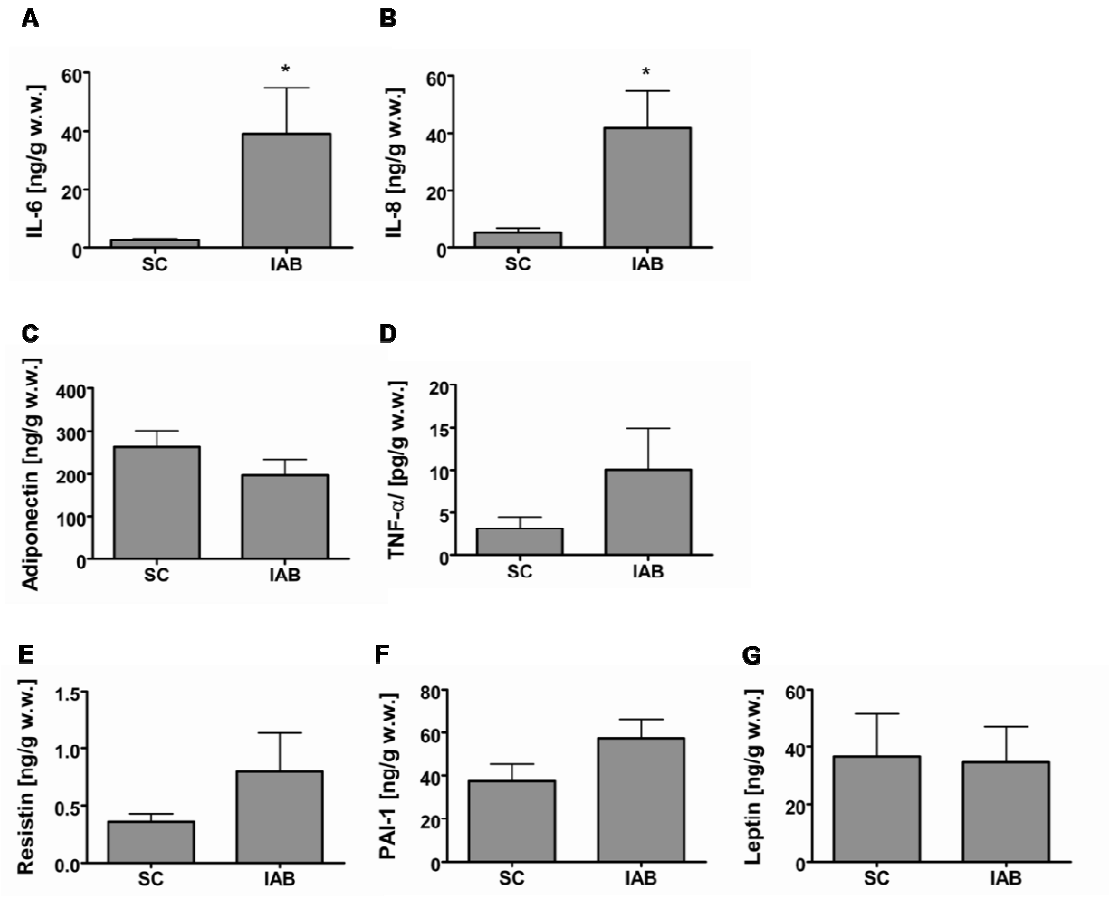

Figure 4.1. Concentrations of adipokines in adipose tissue-conditioned media generated from subcutaneous (SC) and visceral (IAB) fat (n = 4). Concentrations of interleukin (IL)-6 (A), IL-8 (B), adiponectin (C), tumor necrosis factor (TNF)-α (D) resistin (E) and plasminogen activator inhibitor (PAI)-1 (F) were determined using a Human Adipocyte Linco*plex* Kit. The concentration of leptin (G) was measured by ELISA. Data are shown as mean ± SEM. * $P < 0.05$ compared to SC fat.

4.3.2 Fatty acid profiling in the adipose tissue-conditioned medium

The concentration of total fatty acids in CM from SC fat was 1.8-fold higher when compared to that from IAB fat ($P = 0.05$; Figure 4.2A). The difference in the levels of total fatty acids between CM from the two fat depots was mainly attributed to that of *cis*-9 oleic acid (*cis*-9 C18:1), which was 2.4-fold higher in CM from SC fat compared to that from IAB fat ($P < 0.01$; Figure 4.2B). PA (C16:0) and *cis*-9 oleic acid were the two major fatty acids in CM from both fat depots, and when combined contributed to 54% and 59% of the total fatty acids in CM from IAB and SC fat respectively. The percentage of selected fatty acids were not different in CM from the two fat depots except the level of stearic acid (C18:0) which was 1.6-fold ($P < 0.05$) higher while its Δ9 desaturase product, *cis*-9 oleic acid, was significantly lower (83%; $P < 0.05$; Table 4.2) in CM from IAB fat when compared to that from SC fat.

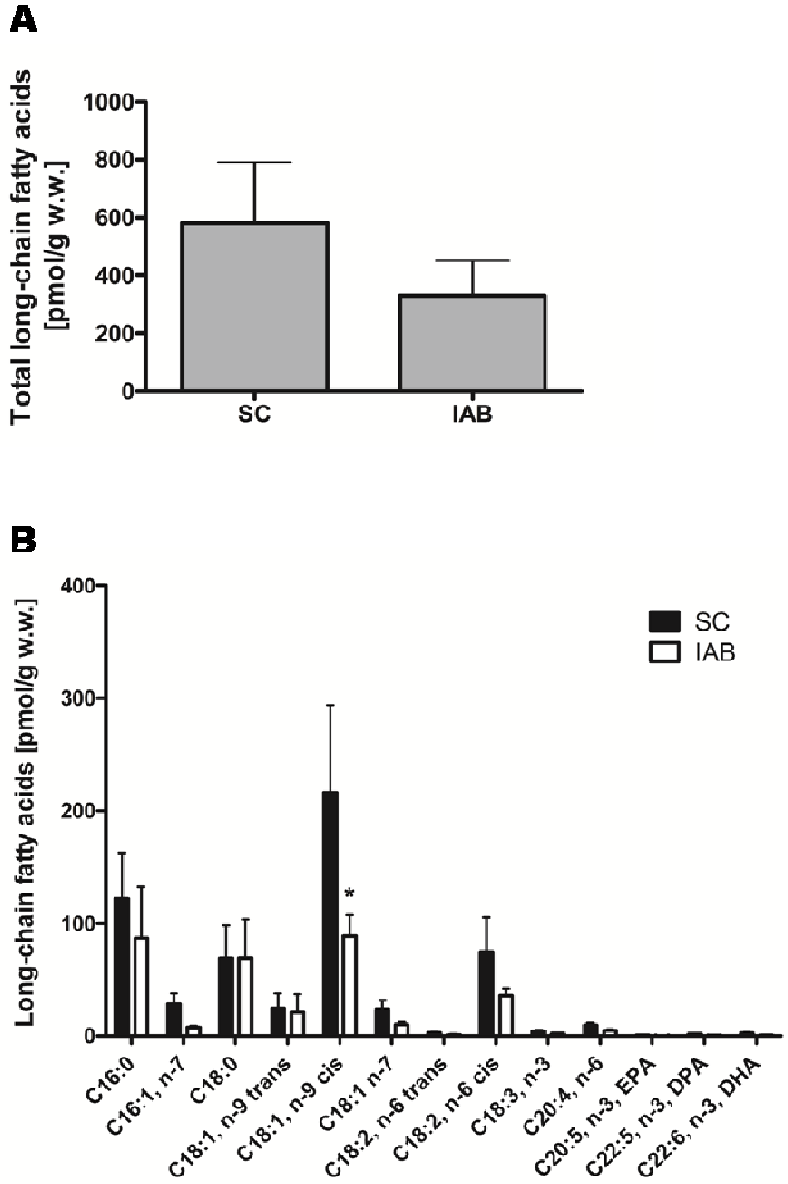

Figure 4.2. Long-chain fatty acids in adipose tissue-conditioned media generated from subcutaneous (SC) and visceral (IAB) fat (n = 4). Concentrations of total (A) and individual (B) long-chain fatty acids were determined using gas chromatography. Data are shown as mean ± SEM. * $P < 0.05$ compared to SC fat. Abbreviations: EPA – eicosapentaenoic acid; DPA – docosapentaenoic acid; DHA – docosahexaenoic acid.

Table 4.2. Molar percentage fatty acid compositions in adipose tissue-conditioned media generated from subcutaneous (SC) and visceral (IAB) fat[3].

Fatty acids[4]	SC fat	IAB fat[5]
C16:0	21.44 ± 1.16	23.17 ± 3.14
C16:1, n-7	4.96 ± 0.46	2.74 ± 0.68
C18:0	11.62 ± 0.94	18.67 ± 2.91 *
C18:1, n-9 trans	3.69 ± 1.15	4.48 ± 1.80
C18:1, n-9 cis	37.37 ± 2.87	30.91 ± 4.09 *
C18:1, n-7	4.38 ± 0.26	3.47 ± 0.57
C18:2, n-6 trans	0.47 ± 0.10	0.37 ± 0.02
C18:2, n-6 cis	12.52 ±0.89	12.60 ± 2.21
C18:3, n-3	0.72 ± 0.04	0.82 ± 0.22
C20:4, n-6	1.90 ± 0.42	2.04 ± 0.53
C20:5, n-3, EPA	0.14 ± 0.03	0.12 ± 0.02
C22:5, n-3, DPA	0.32 ± 0.06	0.24 ± 0.04
C22:6, n-3, DHA	0.49 ± 0.14	0.36 ± 0.07

[3] Values are mean ± SEM, n = 4. Fatty acids are expressed as molar percentages of measured long-chain fatty acids.
[4] Abbreviations: EPA – eicosapentaenoic acid; DPA – docosapentaenoic acid; DHA – docosahexaenoic acid.
[5] * $P < 0.05$ compared to SC fat.

4.3.3 Effect of CM on glucose uptake in L6 myotubes

In the absence of CM (control), insulin induced a 1.6-fold increase in glucose uptake ($P < 0.01$). Basal uptake was not affected by CM from either depot. When compared to the corresponding basal uptake, insulin induced a significant increase in glucose uptake when myotubes were cultured with CM from either fat depots at all concentrations tested ($P < 0.01$). CM from SC fat at concentrations 1:2 – 1:128 had no effect on insulin-stimulated glucose uptake (Figure 4.3A), whereas CM from IAB fat at concentrations of 1:64 and 1:128 resulted in a 14% ($P < 0.05$) and 19% ($P < 0.01$) decrease in insulin-stimulated glucose uptake respectively as compared controls (Figure 4.3B).

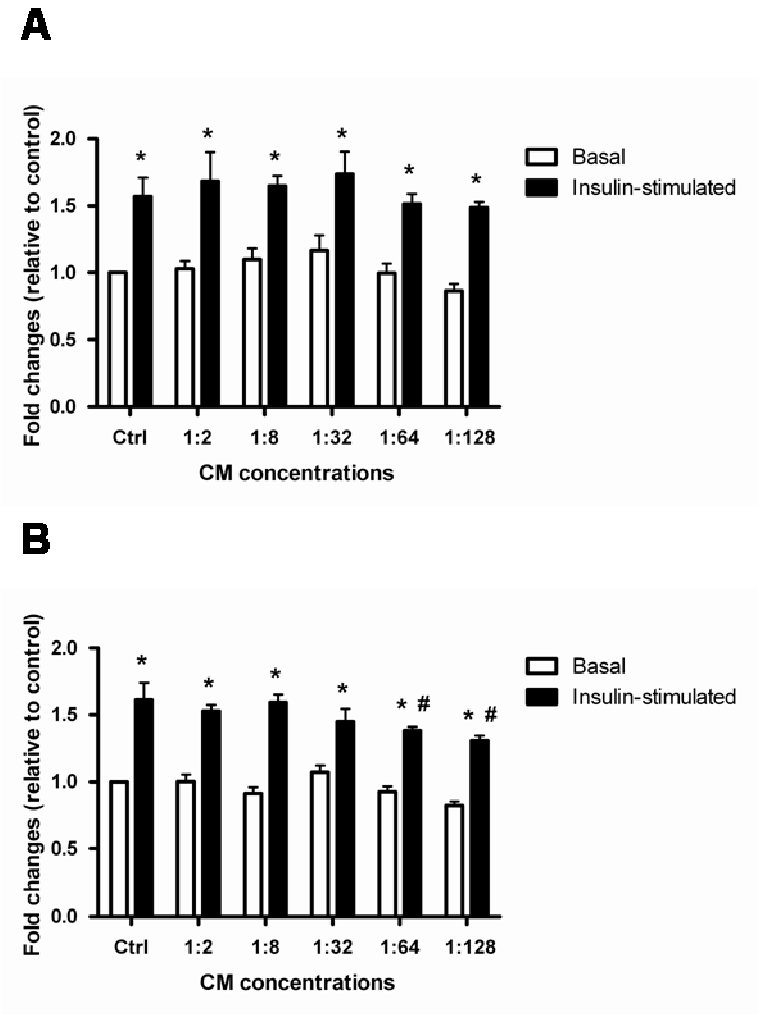

Figure 4.3. The effect of adipose tissue-conditioned media (CM) generated from subcutaneous (A) and visceral (B) fat on basal and insulin-stimulated glucose uptake in L6 myotubes (n = 4). After culturing with conditioned media (concentrations 1:2 – 1:128) for 6 h, L6 myotubes were incubated for 30 min at 37°C in α-MEM with or without insulin (100 nM). Myotubes were then incubated in uptake buffer containing 2-deoxy-D-[^{3}H] glucose (1 μCi/well; 10 μM) for 15 min. Experiments were completed in triplicate. Data are shown as mean ± SEM and are expressed as fold changes relative to the basal uptake in the control (Ctrl). * $P < 0.01$ compared to basal uptake of the corresponding treatment. # $P < 0.05$ compared to the corresponding Ctrl.

4.3.4 Dose-response effect of rapamycin and PDTC on insulin-stimulated glucose uptake in PA-treated myotubes

Rapamycin and PDTC are specific inhibitors of the activation of mTORC1 and NFκB respectively. Rapamycin (40 nM) and PDTC (400 μM) reduced basal glucose uptake by 35% ($P < 0.001$) and 20% ($P < 0.05$) respectively (Figure 4.4). Due to the effect of rapamycin and PDTC on basal uptake, the effect of the inhibitors on insulin action was evaluated by the ratio of insulin-stimulated to basal uptake in the corresponding experimental conditions in subsequent studies. Insulin induced a 27% ($P < 0.01$) increase in glucose uptake, an effect which was abolished by PDTC (Figure 4.4).

The dose-response effect of rapamycin (0 – 40 nM) and PDTC (0 – 400 μM) on insulin-stimulated glucose uptake in PA-treated L6 myotubes was determined. Cytochalasin B-inhibitable basal glucose uptake was undetectable in myotubes treated with 40 nM rapamycin and therefore the data were excluded in the analysis. PA alone abolished the effect of insulin on increasing glucose uptake. There was a trend for rapamycin at 5 – 30 nM to increase insulin-stimulated glucose uptake in PA-treated myotubes and the maximal effect was observed at 20 nM (182%; $P < 0.05$; Figure 4.5A). It should be noted, however, that the magnitude of insulin response was much greater than that usually observed (~ 50%) in this cell line, which raised questions about the validity of the concentrations of both rapamycin (40 nM) and its vehicle DMSO (0.4%; v/v) used in the present study. None of the selected doses of PDTC significantly increased insulin-stimulated glucose uptake in PA-treated myotubes, with the maximal effect in reversing PA-induced insulin resistance observed at 100 μM (79%; $P = 0.34$; Figure 4.5B).

Taken together, 20 nM rapamycin and 100 μM PDTC appeared to be optimal to determine the involvement of mTORC1 and NFκB signalling pathways in skeletal muscle insulin resistance. The effect of rapamycin and PDTC at the selected concentrations was validated in a subsequent study. PA-treated myotubes were incubated with 20 nM rapamycin and 100 μM PDTC and the concentration of DMSO was adjusted to 0.2% (v/v) in all experimental conditions. Rapamycin and PDTC increased insulin-stimulated glucose uptake by 35% *(P* = 0.09) and 32% (*P* = 0.11) respectively (Figure 4.5C). Rapamycin and PDTC, at concentrations of 20 nM and 100 μM respectively, were used in subsequent studies.

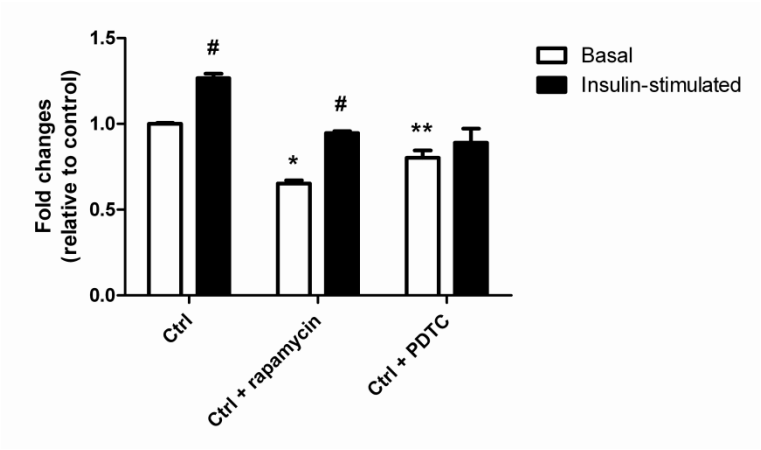

Figure 4.4. The effect of rapamycin and PDTC on basal and insulin-stimulated glucose uptake in L6 myotubes. L6 myotubes were pre-treated with 40 nM rapamycin or 400 μM PDTC for 30 min and the inhibitors were retained during the subsequent 24 h incubation in α-MEM with 0.4% DMSO (v/v), 0.53% BSA (w/v) and 0.08% ethanol (v/v). L6 myotubes were then incubated for 30 min at 37°C in α-MEM with or without insulin (100 nM), followed by incubation in uptake buffer containing 2-deoxy-D-[^{3}H] glucose (1 μCi/well; 10 μM) for 15 min. Experiments were completed in triplicate. Data are expressed as fold changes relative to the basal uptake in the control (Ctrl) and are shown as mean ± SEM. * $P < 0.001$ and ** $P < 0.05$ compared to the corresponding Ctrl. # $P < 0.01$ compared to the corresponding basal uptake.

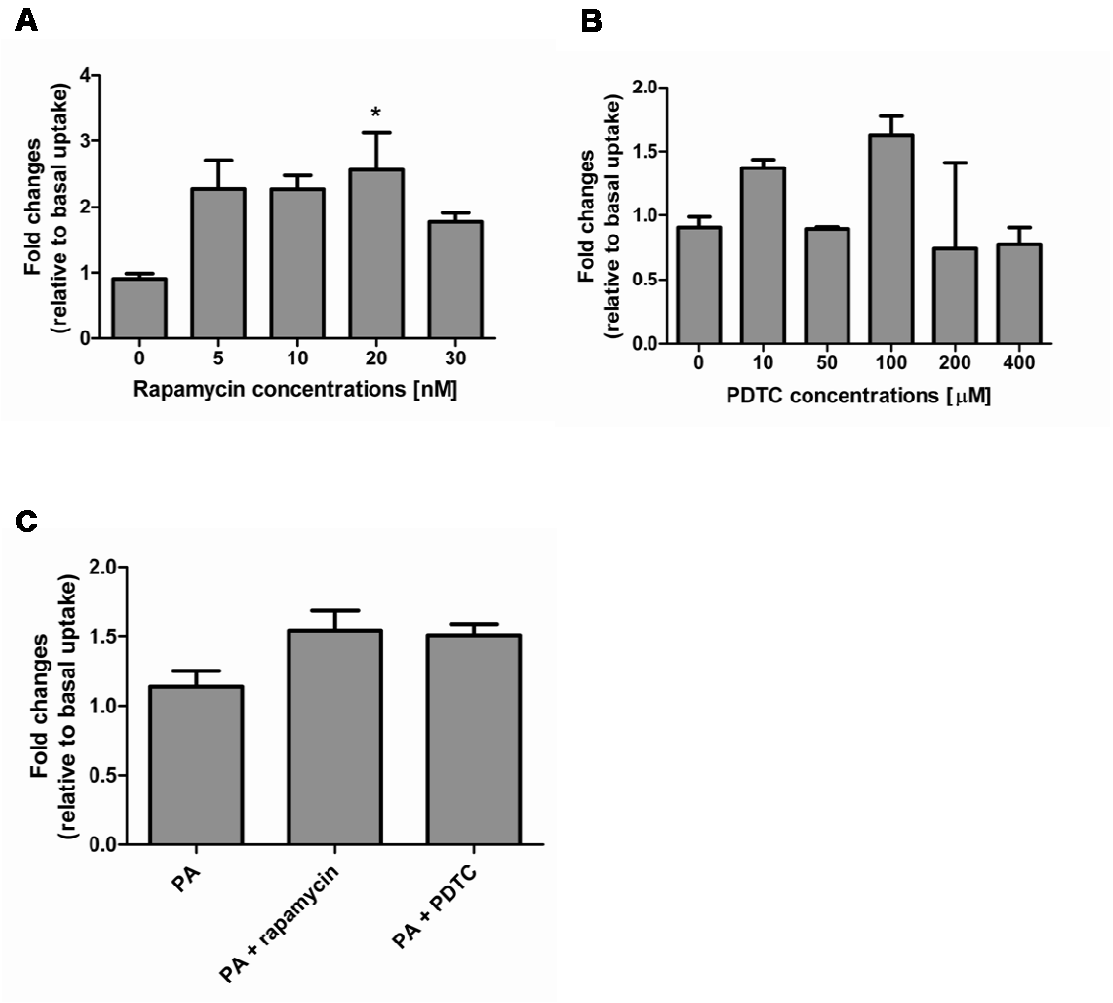

Figure 4.5. Dose-response effect of rapamycin and PDTC on insulin-stimulated glucose uptake in L6 myotubes. L6 myotubes were pre-treated with 0 – 30 nM rapamycin (A), 0 – 400 μM PDTC (B) 20 nM rapamycin and 100 μM PDTC (C) for 30 min and the inhibitors were retained during the subsequent 24 h incubation with palmitic acid (PA). The myotubes were then incubated for 30 min at 37°C in α-MEM with or without insulin (100 nM), followed by incubation in uptake buffer containing 2-deoxy-D-[^{3}H] glucose (1 μCi/well; 10 μM) for 15 min. Experiments were completed in triplicate. Data are expressed as fold changes relative to the corresponding basal uptake and are shown as mean ± SEM. * $P < 0.05$ compared to myotubes cultured with PA alone.

4.3.5 Roles of mTORC1 and NFκB activation in IAB fat-induced insulin resistance in L6 myotubes

In the control cultures, insulin induced a 51% ($P < 0.001$) increase in glucose uptake. CM from IAB fat reduced insulin-stimulated glucose uptake by 25% ($P < 0.01$; Figure 4.6A). When the activation of mTORC1 and NFκB was inhibited, either alone or in combination, the inhibitory effect of CM from IAB fat on insulin-stimulated glucose uptake was completely abolished (Figures 4.6 B to D).

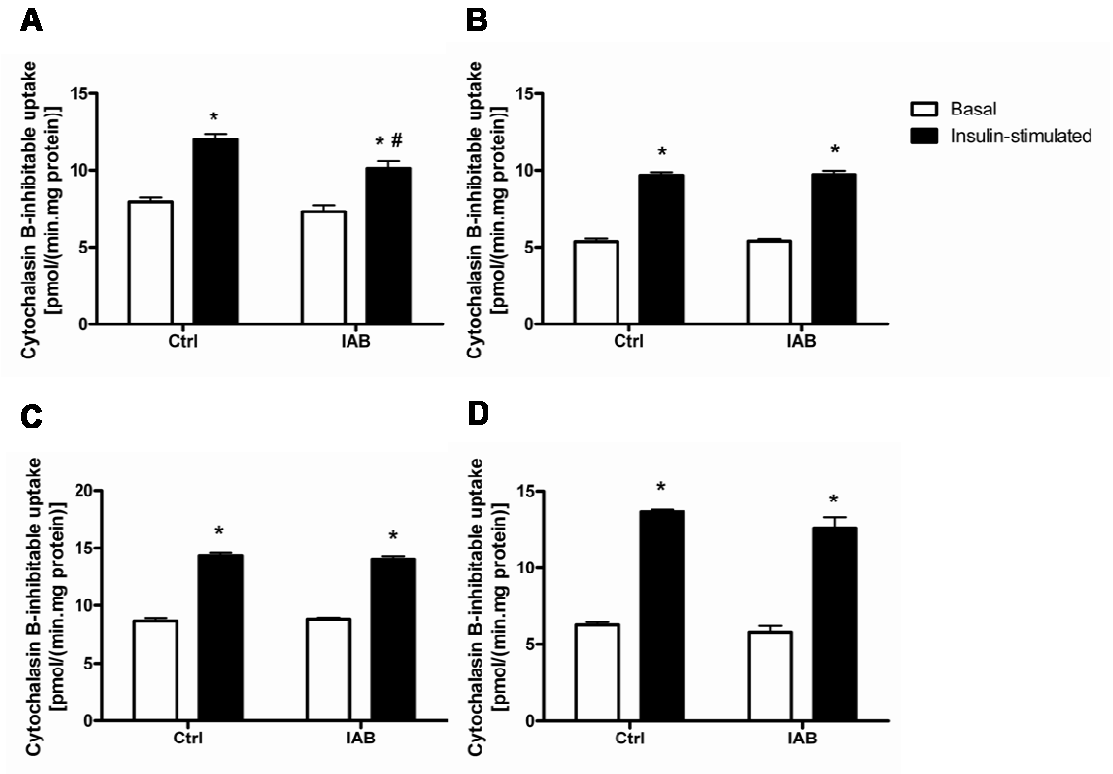

Figure 4.6. The effect of rapamycin and PDTC on basal and insulin-stimulated glucose uptake in L6 myotubes cultured with visceral fat-conditioned media (n = 4). L6 myotubes were pre-treated in the absence of rapamycin and PDTC (A), in the presence of 20 nM rapamycin (B), 100 μM PDTC (C) and a combination of 20 nM rapamycin and 100 μM PDTC (D) for 30 min. The inhibitors were retained when myotubes were cultured in α-MEM with 0.53% BSA (w/v), 0.08% ethanol (v/v) and 0.2% DMSO (v/v) for 24 h with the presence of visceral fat-conditioned media (IAB; concentration 1:128) during the last 6 h of incubation. L6 myotubes were then incubated for 30 min at 37°C in α-MEM with or without insulin (100 nM), followed by incubation in uptake buffer containing 2-deoxy-D-[^{3}H] glucose (1 μCi/well; 10 μM) for 15 min. Experiments were completed in triplicate for each treatment. Data are expressed as fold changes over basal uptake of the corresponding treatment and shown as mean ± SEM. * $P < 0.001$ compared to basal uptake of the corresponding treatment. # $P < 0.01$ compared to insulin-stimulated glucose uptake in the control (Ctrl).

4.3.6 Role of IL-6 in IAB fat-induced insulin resistance in L6 myotubes

The optimal concentration of anti-IL-6 antibody to identify the role of IL-6 in IAB fat-induced insulin resistance in L6 myotubes was determined in a dose-response trial (0 – 40 μg/ml). Compared to myotubes cultured with CM from IAB fat alone, there was a trend for the anti-IL-6 antibody at 1 μg/ml and 10 μg/ml to restore both basal and insulin-stimulated glucose uptake to that of the controls (Figure 4.7). Anti-IL-6 antibody at a concentration of 1 μg/ml or 10 μg/ml was used in the subsequent studies.

In the controls, insulin induced a 42% ($P < 0.01$) increase in glucose uptake in L6 myotubes, which was reduced to 22% ($P < 0.01$) in the presence of CM from IAB fat. Neutralisation of IL-6 in CM from IAB fat using an anti-IL-6 antibody partially restored insulin-stimulated glucose uptake to 65% ($P = 0.24$) of the controls (Figure 4.8).

The role of IL-6 in mediating IAB fat-induced insulin resistance was further verified by incubating L6 myotubes with human recombinant IL-6 (#CYT-213, Pro-Spec-Tany TechnoGene, Rehovot, Israel) at concentrations comparable to those in CM from 4 donors (43.5 ± 17.0 pg/ml, range 6.7 – 88.3 pg/ml). IL-6 inhibited insulin-stimulated glucose uptake in a dose-dependent manner by up to 72% ($P < 0.001$; Figure 4.9A). IL-6 at a concentration of 50 pg/ml (a dose similar to the average IL-6 concentration in CM from IAB fat) reduced insulin-stimulated glucose uptake by 53% ($P < 0.05$), an effect that was completely abolished by either neutralising IL-6 (Figure 4.9B) or inhibiting the activation of mTORC1 or NFκB (Figure 4.10).

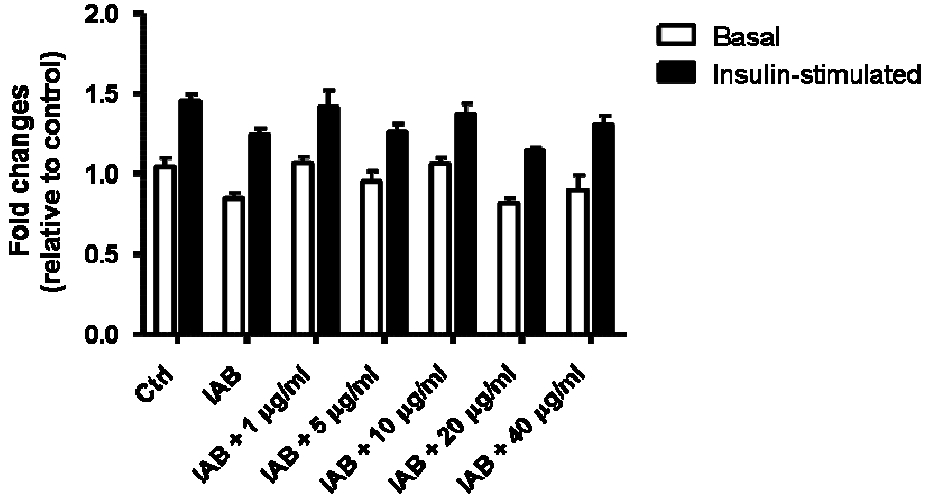

Figure 4.7. Dose-response effect of anti-interleukin (IL)-6 antibody on basal and insulin-stimulated glucose uptake in L6 myotubes cultured with visceral fat-conditioned media (n = 2). L6 myotubes were cultured with conditioned media generated from visceral fat (IAB; concentration 1:128) for 6 h in the presence of an anti-IL-6 antibody (0 – 40 µg/ml). L6 myotubes were then incubated for 30 min at 37°C in α-MEM with or without insulin (100 nM), followed by incubation in uptake buffer containing 2-deoxy-D-[^{3}H] glucose (1 µCi/well; 10 µM) for 15 min. Experiments were repeated in triplicate for each treatment. Data are expressed as fold changes relative to the basal uptake of the control (Ctrl).

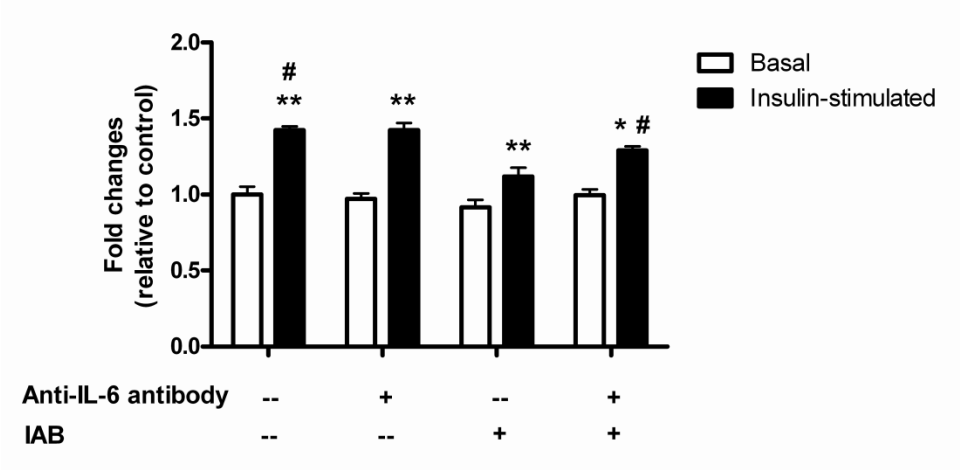

Figure 4.8. The effect of interleukin (IL)-6 neutralisation on basal and insulin-stimulated glucose uptake in L6 myotubes cultured with visceral fat-conditioned media (n = 4). L6 myotubes were cultured with conditioned media generated from visceral fat (IAB; concentration 1:128) for 6 h in the presence of 1 μg/ml anti-IL-6 antibody. L6 myotubes were then incubated for 30 min at 37°C in α-MEM with or without insulin (100 nM), followed by incubation in uptake buffer containing 2-deoxy-D-[^{3}H] glucose (1 μCi/well; 10 μM) for 15 min. Experiments were completed in triplicate for each treatment. Data are expressed as fold changes over basal control. * $P < 0.001$ and ** $P < 0.01$ compared to the basal uptake of the corresponding treatment. # $P < 0.01$ compared to insulin-stimulated uptake in IAB fat-treated myotubes.

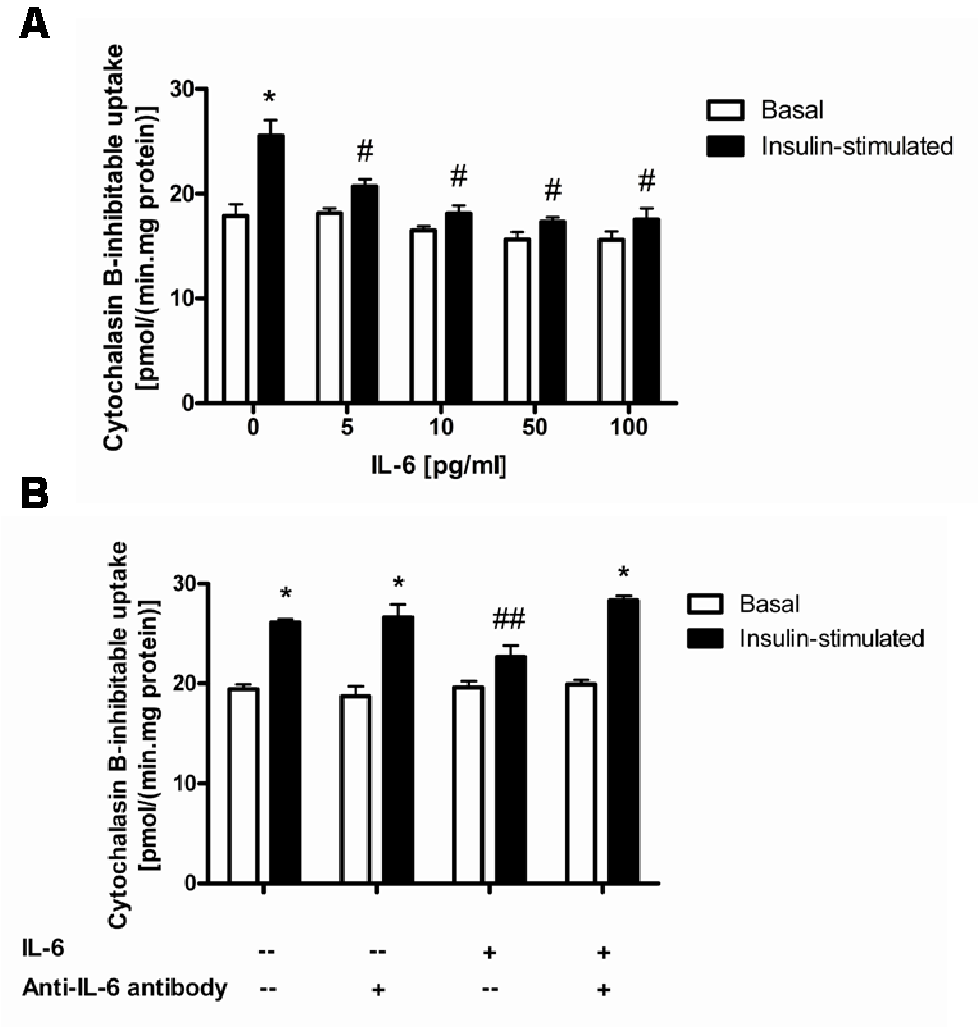

Figure 4.9. The effect of interleukin (IL)-6 on basal and insulin-stimulated glucose uptake in L6 myotubes. L6 myotubes were cultured with 0 – 100 pg/ml (A) and 50 pg/ml IL-6 with or without 10 μg/ml anti-IL-6 antibody (B) for 6 h. L6 myotubes were then incubated for 30 min at 37°C in α-MEM with or without insulin (100 nM), followed by incubation in uptake buffer containing 2-deoxy-D-[^{3}H] glucose (1 μCi/well; 10 μM) for 15 min. Experiments were completed in triplicate for each treatment. Data are shown as mean ± SEM. * $P < 0.001$ compared to the basal uptake of the corresponding treatment. # $P < 0.001$ and ## $P < 0.05$ compared to insulin-stimulated uptake in the corresponding control.

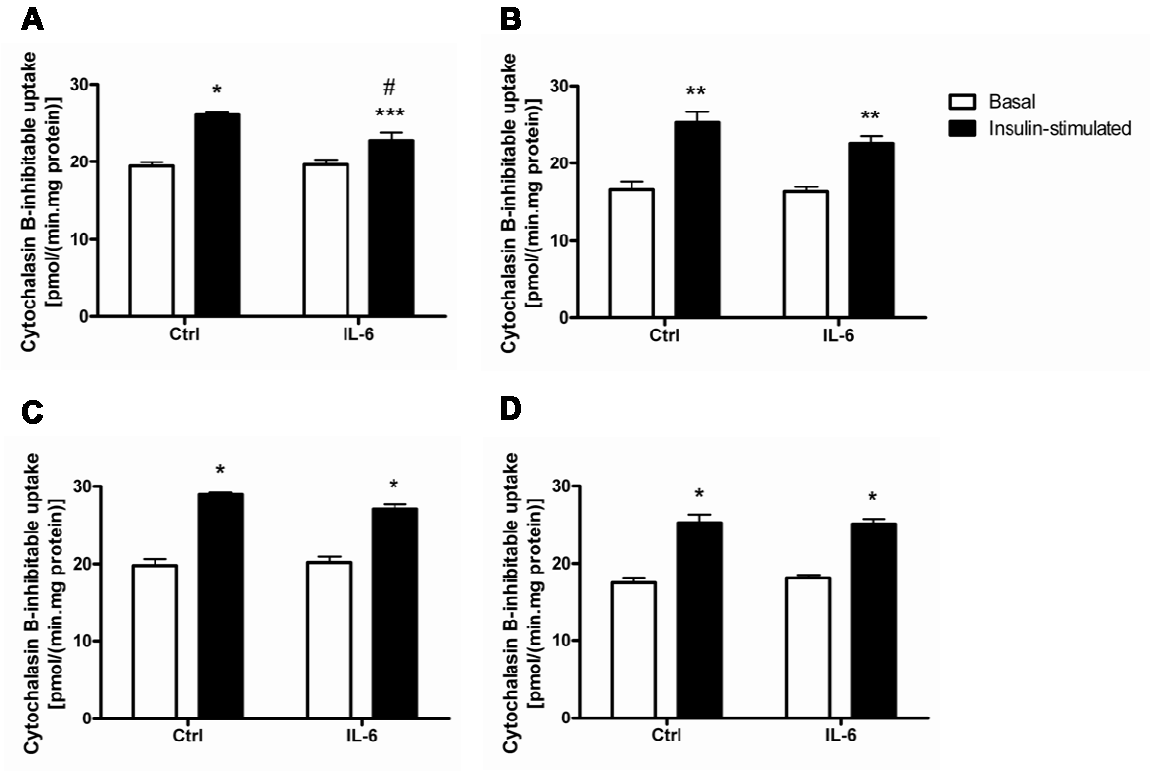

Figure 4.10. The effect of rapamycin and PDTC on basal and insulin-stimulated glucose uptake in L6 myotubes cultured with interleukin (IL)-6. L6 myotubes were pre-treated in the absence of rapamycin and PDTC (A), in the presence of 20 nM rapamycin (B), 100 μM PDTC (C) and a combination of 20 nM rapamycin and 100 μM PDTC (D) for 30 min. The inhibitors were retained when myotubes were cultured with 50 pg/ml IL-6 for 6 h. L6 myotubes were then incubated for 30 min at 37°C in α-MEM with or without insulin (100 nM), followed by incubation in uptake buffer containing 2-deoxy-D-[^{3}H] glucose (1 μCi/well; 10 μM) for 15 min. Experiments were completed in triplicate for each treatment. Data are shown as mean ± SEM. * $P < 0.001$, ** $P < 0.01$ and *** $P < 0.05$ compared to basal uptake of the corresponding treatment. # $P < 0.05$ compared to insulin-stimulated uptake in the control (Ctrl).

4.4 Discussion

The present study demonstrated the depot-specific effect of adipose tissue on insulin sensitivity in skeletal muscle *in vitro*. The net effect of secretory factors from IAB but not SC fat reduced insulin-stimulated glucose uptake in L6 myotubes. The inhibitory effect of CM from IAB fat on insulin-stimulated glucose uptake was only observed at low concentrations (1:64 and 1:128). This may be due to the combined effect of cytokines with opposing actions on the mechanisms regulating muscle insulin sensitivity. In CM at high concentrations, the effect of pro-inflammatory cytokines on reducing insulin-stimulated glucose uptake in L6 myotubes may be neutralised by the insulin-sensitising effects of leptin and adiponectin. When CM from IAB fat was diluted, the inhibitory effect of pro-inflammatory cytokines on insulin-stimulated glucose uptake in skeletal muscle cells seemed to predominate. This highlights the effect of complex interactions between cytokines from the adipose tissue and the importance of establishing and validating the co-culture system under specific conditions.

Obesity is characterised by an increased release of fatty acids from the adipose tissue to the portal and systemic circulations (Wajchenberg 2000). The increased fatty acid flux to non-adipose tissues, in particular liver, muscle and pancreatic β-cells, may lead to obesity-related metabolic abnormalities. In the present study, the concentration of long-chain fatty acids in CM from SC fat was 1.8-fold higher when compared to that from IAB fat, an observation consistent with the previously documented higher basal rate of lipolysis in SC as compared to IAB fat (Tchernof et al. 2006). The overall fatty acid profile in the CM reflected the composition of the average dietary fatty acid intake and the tissue fatty acid profile as previously reported (Vessby et al. 2002). The two major dietary saturated fatty acids, PA and stearic acid, together contributed to 33% and 42% of

the total fatty acids in CM from SC and IAB fat respectively. *Cis*-9 oleic acid, the main monounsaturated fatty acid in the Western diet, was the most abundant fatty acid in CM from both fat depots. When compared to CM from IAB fat, CM from SC fat had lower proportions of stearic acid and higher *cis*-9 oleic acid. A possible explanation may be a higher SCD activity in SC compared to IAB adipose tissue. Sjögren et al (2008) reported that insulin-resistant individuals had a higher 18:1/18:0 ratio in SC fat than their insulin-sensitive counterparts and the increased SCD activity in adipose tissue was related to insulin resistance. The similar overall fatty acid profile in CM from IAB and SC fat also suggest intramuscular accumulation of lipid metabolites is unlikely to mediate IAB fat-induced insulin resistance in skeletal muscle cells.

The effect of CM from IAB fat on reducing insulin-stimulated glucose uptake in L6 myotubes may be a consequence of an increased release of pro-inflammatory cytokines from the fat depot. In accordance with regional differences in adipokine production documented previously, CM from IAB fat contained higher concentrations of pro-inflammatory cytokines including IL-6 (Bruun et al. 2004), IL-8 (Bruun et al. 2004), TNF-α (Orel et al. 2004), resistin (Fain et al. 2003) and PAI-1 (Fain et al. 2004), as compared to SC fat. Previous studies have shown that cells in the stromal-vascular fraction of the adipose tissue, including preadipocytes, endothelial cells and monocytes-macrophages, play a major role in the production of pro-inflammatory cytokines in this tissue. Only 10% of IL-6 released by adipose tissue explants was accounted for by isolated adipocytes (Fried et al. 1998). The stromal-vascular fraction has been shown to produce 7- to 8-fold more IL-8 compared to adipocytes (Bruun et al. 2005). Resistin was predominantly released by the white adipose tissue-derived macrophages (Curat et al. 2006), and PAI-1 from stromal-vascular cells (Bastelica et al. 2002).

Although not measured in the present study, differential infiltration, and in particular activation, of macrophages in SC and IAB fat may explain the depot-specific adipokine secretion profile and provides a direct link between inflammation and insulin resistance in obesity. Increased infiltrated macrophages in omental as compared to subcutaneous fat has been consistently demonstrated (Cancello et al. 2006; Harman-Boehm et al. 2007). Resting macrophages, however, release low levels of pro-inflammatory cytokines and the expression of these proteins are only up-regulated when the macrophages are in the activated state (Ortega Martinez de Victoria et al. 2009). In addition to the increased abundance of infiltrated macrophages, the higher expression of MCP-1, a cytokine capable of inducing macrophage migration and activation (Yu et al. 2006), in IAB compared to SC fat further supports the role of activated macrophages in IAB fat in the release of pro-inflammatory cytokines (Bruun et al. 2005).

The effect of CM from IAB fat on reducing insulin-stimulated glucose uptake in L6 myotubes was completely reversed by inhibiting the activation of either NFκB or mTORC1. The inhibitory effect of individual pro-inflammatory cytokines, including TNF-α (Borst et al. 2004; de Alvaro et al. 2004) and IL-6 (Kim et al. 2004; Nieto-Vazquez et al. 2008) on insulin sensitivity in skeletal muscle has been consistently demonstrated in *in vivo* and *in vitro*. While these pro-inflammatory cytokines all inhibit insulin signal transduction by serine phosphorylation of IRS-1, these data suggest that there may be a point of convergence for inflammation-induced insulin resistance. Adipokines including TNF-α, IL-1 and IL-6 are known inducers of NFκB activation (Lee and Burckart 1998; Lam et al. 2008). The activation of NFκB induces gene transcription of pro-inflammatory cytokines which subsequently results in a positive-feedback loop that further activates the IKK/IκB/NFκB pathway (Lee and Burckart 1998). mTORC1

activation may act downstream of the IKK/IκB/NFκB pathway which mediates the inhibitory effect of pro-inflammatory cytokines on insulin signalling. IKK phosphorylates TSC-1 and thus activates mTORC1 (Lee et al. 2008). S6K1 is the downstream substrate of mTORC1 which, when activated, has been shown to induce serine phosphorylation of IRS-1 in HepG2 cells (Kim et al. 2008) and adipocytes (Zhang et al. 2008). Aspirin, a specific IKK inhibitor, prevented TNF-α-induced phosphorylation of S6K1 in 3T3-L1 adipocytes (Gao et al. 2003).

Taken together, a NFκB/mTORC1-dependent pathway may induce insulin resistance and support the role of pro-inflammatory cytokines in mediating the inhibitory effect of IAB fat on insulin-stimulated glucose uptake in L6 myotubes. In particular, the present data suggest that IL-6 is a major adipokine that mediates the effect of IAB fat, which by itself reduced insulin-stimulated glucose uptake in L6 myotubes via the NFκB/mTORC1-dependent pathway. The effect of CM from IAB fat on reducing insulin responsiveness was completely reversed by inhibiting the activation of either NFκB or mTORC1 but was only partially reversed by neutralising IL-6. Accordingly, other pro-inflammatory cytokines from IAB fat must account for the overall effect of IAB fat-induced insulin resistance in skeletal muscle cells.

In addition to pro-inflammatory cytokines which may induce insulin resistance, adipose tissue also releases cytokines which have an insulin-sensitising effect. Leptin and adiponectin have been shown to increase insulin sensitivity in skeletal muscle via the phosphorylation of AMPK (Fruhbeck and Salvador 2000; Karbowska and Kochan 2006). In contrast to the greater release of pro-inflammatory cytokines, resistin and PAI-1 from visceral fat, the concentration of adiponectin were 1.3-fold greater in CM from SC fat as

compared to IAB fat, an observation consistent with the known depot-specific difference from studies in cultured adipocytes (Grohmann et al. 2005). In contrast there was no difference in the levels of leptin between CM from the two fat depots. A possible reason for this discrepancy may be the disproportion of female and male donors (three females and one male) in the present study. Gender-specific differences have been demonstrated previously with plasma leptin levels higher in females than in males in both healthy and obese individuals (Baratta et al. 2004). *In vitro*, adipose tissue from female donors releases greater amounts of leptin than those from male donors (Casabiell et al. 1998). Samples from a mixed group of donors may have offset the anticipated difference in leptin concentrations in CM from SC and IAB fat.

In summary, the characteristics of CM including the fatty acid and cytokine profiles, together with the effects of CM on insulin-stimulated glucose uptake in skeletal muscle cells, confirmed the physiological relevance and utility of adipose tissue-conditioned media to determine the effect of adipose tissue-skeletal muscle interactions. This model facilitates the study of the involvement of individual cytokines, as well as their interactions and the mechanisms by which they occur, in visceral fat-induced muscle insulin resistance and may also assist in understanding the complex metabolic interactions between different adipose tissue depots and other aspects of skeletal muscle energy metabolism. The data demonstrate that secretory factors from IAB fat reduced insulin-stimulated glucose uptake in skeletal muscle cells, while those from SC fat were without effect. I proposed that the IAB fat-induced insulin resistance was at least in part mediated by pro-inflammatory cytokines, in particular IL-6, via the activation of a NFκB/mTORC1-dependent pathway.